Title	Determination of the number of J/ψ events with J/ψ → inclusive decays

Determination of the number of J/ψ events with $J/\psi \to$ *inclusive* decays

M. Ablikim[1], M. N. Achasov[5], D. J. Ambrose[40], F. F. An[1], Q. An[41], Z. H. An[1], J. Z. Bai[1], Y. Ban[27], J. Becker[2], N. Berger[1], M. Bertani[18], J. M. Bian[39], E. Boger[20a], O. Bondarenko[21], I. Boyko[20], R. A. Briere[3], V. Bytev[20], X. Cai[1], A. Calcaterra[18], G. F. Cao[1], J. F. Chang[1], G. Chelkov[20a], G. Chen[1], H. S. Chen[1], J. C. Chen[1], M. L. Chen[1], S. J. Chen[25], Y. Chen[1], Y. B. Chen[1], H. P. Cheng[14], Y. P. Chu[1], D. Cronin-Hennessy[39], H. L. Dai[1], J. P. Dai[1], D. Dedovich[20], Z. Y. Deng[1], A. Denig[19], I. Denysenko[20b], M. Destefanis[43], W. M. Ding[29], Y. Ding[23], L. Y. Dong[1], M. Y. Dong[1], S. X. Du[46], J. Fang[1], S. S. Fang[1], L. Fava[43c], F. Feldbauer[2], C. Q. Feng[41], R. B. Ferroli[18], C. D. Fu[1], J. L. Fu[25], Y. Gao[36], C. Geng[41], K. Goetzen[7], W. X. Gong[1], W. Gradl[19], M. Greco[43], M. H. Gu[1], Y. T. Gu[9], Y. H. Guan[6], A. Q. Guo[26], L. B. Guo[24], Y.P. Guo[26], Y. L. Han[1], X. Q. Hao[1], F. A. Harris[38], K. L. He[1], M. He[1], Z. Y. He[26], T. Held[2], Y. K. Heng[1], Z. L. Hou[1], H. M. Hu[1], J. F. Hu[6], T. Hu[1], B. Huang[1], G. M. Huang[15], J. S. Huang[12], X. T. Huang[29], Y. P. Huang[1], T. Hussain[42], C. S. Ji[41], Q. Ji[1], X. B. Ji[1], X. L. Ji[1], L. K. Jia[1], L. L. Jiang[1], X. S. Jiang[1], J. B. Jiao[29], Z. Jiao[14], D. P. Jin[1], S. Jin[1], F. F. Jing[36], N. Kalantar-Nayestanaki[21], M. Kavatsyuk[21], W. Kuehn[37], W. Lai[1], J. S. Lange[37], J. K. C. Leung[35], C. H. Li[1], Cheng Li[41], Cui Li[41], D. M. Li[46], F. Li[1], G. Li[1], H. B. Li[1], J. C. Li[1], K. Li[10], Lei Li[1], N. B. Li[24], Q. J. Li[1], S. L. Li[1], W. D. Li[1], W. G. Li[1], X. L. Li[29], X. N. Li[1], X. Q. Li[26], X. R. Li[28], Z. B. Li[33], H. Liang[41], Y. F. Liang[31], Y. T. Liang[37], G. R. Liao[36], X. T. Liao[1], B. J. Liu[1, 34], C. L. Liu[3], C. X. Liu[1], C. Y. Liu[1], F. H. Liu[30], Fang Liu[1], Feng Liu[15], H. Liu[1], H. B. Liu[6], H. H. Liu[13], H. M. Liu[1], H. W. Liu[1], J. P. Liu[44], K. Y. Liu[23], Kai Liu[6], Kun Liu[27], P. L. Liu[29], S. B. Liu[41], X. Liu[22], X. H. Liu[1], Y. Liu[1], Y. B. Liu[26], Z. A. Liu[1], Zhiqiang Liu[1], Zhiqing Liu[1], H. Loehner[21], G. R. Lu[12], H. J. Lu[14], J. G. Lu[1], Q. W. Lu[30], X. R. Lu[6], Y. P. Lu[1], C. L. Luo[24], M. X. Luo[45], T. Luo[38], X. L. Luo[1], M. Lu[1], C. L. Ma[6], F. C. Ma[23], H. L. Ma[1], Q. M. Ma[1], S. Ma[1], T. Ma[1], X. Y. Ma[1], Y. Ma[11], F. E. Maas[11], M. Maggiora[43], Q. A. Malik[42], H. Mao[1], Y. J. Mao[27], Z. P. Mao[1], J. G. Messchendorp[21], J. Min[1], T. J. Min[1], R. E. Mitchell[17], X. H. Mo[1], C. Morales Morales[11], C. Motzko[2], N. Yu. Muchnoi[5], Y. Nefedov[20], C. Nicholson[6], I. B. Nikolaev[5], Z. Ning[1], S. L. Olsen[28], Q. Ouyang[1], S. Pacetti[18d], J. W. Park[28], M. Pelizaeus[38], H. P. Peng[41], K. Peters[7], J. L. Ping[24], R. G. Ping[1], R. Poling[39], E. Prencipe[19], C. S. J. Pun[35], M. Qi[25], S. Qian[1], C. F. Qiao[6], X. S. Qin[1], Y. Qin[27], Z. H. Qin[1], J. F. Qiu[1], K. H. Rashid[42], G. Rong[1], X. D. Ruan[9], A. Sarantsev[20e], B. D. Schaefer[17], J. Schulze[2], M. Shao[41], C. P. Shen[38f], X. Y. Shen[1], H. Y. Sheng[1], M. R. Shepherd[17], X. Y. Song[1], S. Spataro[43], B. Spruck[37], D. H. Sun[1], G. X. Sun[1], J. F. Sun[12], S. S. Sun[1], X. D. Sun[1], Y. J. Sun[41], Y. Z. Sun[1], Z. J. Sun[1], Z. T. Sun[41], C. J. Tang[31], X. Tang[1], E. H. Thorndike[40], H. L. Tian[1], D. Toth[39], M. Ullrich[37], G. S. Varner[38], B. Wang[9], B. Q. Wang[27], K. Wang[1], L. L. Wang[4], L. S. Wang[1], M. Wang[29], P. Wang[1], P. L. Wang[1], Q. Wang[1], Q. J. Wang[1], S. G. Wang[27], X. F. Wang[12], X. L. Wang[41], Y. D. Wang[41], Y. F. Wang[1], Y. Q. Wang[29], Z. Wang[1], Z. G. Wang[1], Z. Y. Wang[1], D. H. Wei[8], P. Weidenkaff[19], Q. G. Wen[41], S. P. Wen[1], M. Werner[37], U. Wiedner[2], L. H. Wu[1], N. Wu[1], S. X. Wu[41], W. Wu[26], Z. Wu[1], L. G. Xia[36], Z. J. Xiao[24], Y. G. Xie[1], Q. L. Xiu[1], G. F. Xu[1], G. M. Xu[27], H. Xu[1], Q. J. Xu[10], X. P. Xu[32], Y. Xu[26], Z. R. Xu[41], F. Xue[15], Z. Xue[1], L. Yan[41], W. B. Yan[41], Y. H. Yan[16], H. X. Yang[1], T. Yang[9], Y. Yang[15], Y. X. Yang[8], H. Ye[1], M. Ye[1], M. H. Ye[4], B. X. Yu[1], C. X. Yu[26], J. S. Yu[22], S. P. Yu[29], C. Z. Yuan[1], W. L. Yuan[24], Y. Yuan[1], A. A. Zafar[42], A. Zallo[18], Y. Zeng[16], B. X. Zhang[1], B. Y. Zhang[1], C. C. Zhang[1], D. H. Zhang[1], H. H. Zhang[33], H. Y. Zhang[1], J. Zhang[24], J. G. Zhang[12], J. Q. Zhang[1], J. W. Zhang[1], J. Y. Zhang[1], J. Z. Zhang[1], L. Zhang[25], S. H. Zhang[1], T. R. Zhang[24], X. J. Zhang[1], X. Y. Zhang[29], Y. Zhang[1], Y. H. Zhang[1], Y. S. Zhang[9], Z. P. Zhang[41], Z. Y. Zhang[44], G. Zhao[1], H. S. Zhao[1], J. W. Zhao[1], K. X. Zhao[24], Lei Zhao[41], Ling Zhao[1], M. G. Zhao[26], Q. Zhao[1], S. J. Zhao[46], T. C. Zhao[1], X. H. Zhao[25], Y. B. Zhao[1], Z. G. Zhao[41], A. Zhemchugov[20a], J. P. Zheng[1], Y. H. Zheng[6], Z. P. Zheng[1], B. Zhong[1], J. Zhong[2], L. Zhou[1], X. K. Zhou[6], X. R. Zhou[41], C. Zhu[1], K. Zhu[1], K. J. Zhu[1], S. H. Zhu[1], X. L. Zhu[36], X. W. Zhu[1], Y. M. Zhu[26], Y. S. Zhu[1], Z. A. Zhu[1], J. Zhuang[1], B. S. Zou[1], J. H. Zou[1], J. X. Zuo[1]

[1] *Institute of High Energy Physics, Beijing 100049, China*
[2] *Bochum Ruhr-University, 44780 Bochum, Germany*
[3] *Carnegie Mellon University, Pittsburgh, PA 15213, USA*
[4] *China Center of Advanced Science and Technology, Beijing 100190, China*
[5] *G.I. Budker Institute of Nuclear Physics SB RAS (BINP), Novosibirsk 630090, Russia*
[6] *Graduate University of Chinese Academy of Sciences, Beijing 100049, China*
[7] *GSI Helmholtzcentre for Heavy Ion Research GmbH, D-64291 Darmstadt, Germany*
[8] *Guangxi Normal University, Guilin 541004, China*

[9] GuangXi University, Nanning 530004, China
[10] Hangzhou Normal University,
Hangzhou 310036, China
[11] Helmholtz Institute Mainz,
J.J. Becherweg 45,D 55099 Mainz, Germany
[12] Henan Normal University, Xinxiang 453007, China
[13] Henan University of Science and Technology,
Luoyang 471003, China
[14] Huangshan College, Huangshan 245000, China
[15] Huazhong Normal University, Wuhan 430079, China
[16] Hunan University, Changsha 410082, China
[17] Indiana University, Bloomington, Indiana 47405, USA
[18] INFN Laboratori Nazionali di Frascati , Frascati, Italy
[19] Johannes Gutenberg University of Mainz,
Johann-Joachim-Becher-Weg 45, 55099 Mainz, Germany
[20] Joint Institute for Nuclear Research,
141980 Dubna, Russia
[21] KVI/University of Groningen,
9747 AA Groningen, The Netherlands
[22] Lanzhou University, Lanzhou 730000, China
[23] Liaoning University, Shenyang 110036, China
[24] Nanjing Normal University, Nanjing 210046, China
[25] Nanjing University, Nanjing 210093, China
[26] Nankai University, Tianjin 300071, China
[27] Peking University, Beijing 100871, China
[28] Seoul National University, Seoul, 151-747 Korea
[29] Shandong University, Jinan 250100, China
[30] Shanxi University, Taiyuan 030006, China
[31] Sichuan University, Chengdu 610064, China
[32] Soochow University, Suzhou 215006, China
[33] Sun Yat-Sen University, Guangzhou 510275, China
[34] The Chinese University of Hong Kong,
Shatin, N.T., Hong KongChina
[35] The University of Hong Kong,
Pokfulam, Hong Kong, China
[36] Tsinghua University, Beijing 100084, China
[37] Universitaet Giessen, 35392 Giessen, Germany
[38] University of Hawaii, Honolulu, Hawaii 96822, USA
[39] University of Minnesota,
Minneapolis, MN 55455, USA
[40] University of Rochester,
Rochester, New York 14627, USA
[41] University of Science and Technology of China,
Hefei 230026, China
[42] University of the Punjab, Lahore-54590, Pakistan
[43] University of Turin and INFN, Turin, Italy
[44] Wuhan University, Wuhan 430072, China
[45] Zhejiang University, Hangzhou 310027, China
[46] Zhengzhou University, Zhengzhou 450001, China
[a] also at the Moscow Institute of Physics and Technology, Moscow, Russia
[b] on leave from the Bogolyubov Institute for Theoretical Physics, Kiev, Ukraine
[c] University of Piemonte Orientale and INFN (Turin)
[d] University of Perugia and INFN, I-06100 Perugia, Italy
[e] also at the PNPI, Gatchina, Russia
[f] now at Nagoya University, Nagoya, Japan

(BESIII Collaboration)

The number of J/ψ events collected with the BESIII detector at the BEPCII from June 12 to July 28, 2009 is determined to be $(225.3 \pm 2.8) \times 10^6$ using $J/\psi \to inclusive$ events, where the uncertainty is the systematic error and the statistical one is negligible.

I. INTRODUCTION

To meet the challenge of precision measurements of $\tau-$charm physics, a major upgrade on the Beijing Electron-Positron Collider (BEPC) and the Beijing Spec-

trometer (BES) was completed in 2008 (now called BEPCII and BESIII). BEPCII is a double ring e^+e^- collider with a design peak luminosity of 10^{33} cm$^{-2}s^{-1}$ at $\sqrt{s}$ =3.773 GeV, which is 100 times that of its predecessor. The BESIII detector is a large solid-angle magnetic spectrometer that is described in detail in Ref. [1]. The major improvements in the BES detector are the huge superconducting solenoid magnet with a central field of 1 T, which offers a significant improvement in the momentum resolution of charged particles, and a cesium iodide (CsI) calorimeter for the energy measurement of electrons and photons, which provides more than a factor of 10 improvement in the precision of electromagnetic shower energy measurements.

Since the discovery of the J/ψ in 1974, it has always been regarded as an ideal laboratory to study light hadron spectroscopy and to search for new types of hadrons (e.g. glueballs, hybrids and exotics). With 58 million J/ψ events collected with the BESII detector, many important results have been obtained, which underlined the importance of the study of J/ψ decays. Therefore, after a successful commissioning of the BESIII detector together with BEPCII, a large sample of J/ψ events was collected from June 12 to July 28, 2009, which allows the study of the properties and the decays of the J/ψ with unprecedented precision.

The number of J/ψ events and its uncertainty are two key quantities in the precision measurements of J/ψ decays. At BESII, the number of J/ψ events was determined with $J/\psi \to$ 4-prong events, and its systematic uncertainty was 4.7% [2]. The excellent BESIII detector and its good performance allow the determination of the number of J/ψ events with higher precision. To reduce the systematic uncertainty from that in Ref. [2], a new method using $J/\psi \to inclusive$ events is introduced. The number of J/ψ events ($N_{J/\psi}$) is calculated with

$$N_{J/\psi} = \frac{N_{sel} - N_{bg}}{\epsilon_{trig} \times \epsilon^{\psi'}_{data} \times f_{cor}}, \quad (1)$$

where N_{sel} is the number of $J/\psi \to inclusive$ events selected from J/ψ data; N_{bg} is the number of background events estimated from the continuum data taken at the center-of-mass energy of 3.08 GeV; ϵ_{trig} is the trigger efficiency; $\epsilon^{\psi'}_{data}$ is the $J/\psi \to inclusive$ detection efficiency determined experimentally from ψ' data using $\psi' \to \pi^+\pi^- J/\psi$ events; f_{cor} is a correction factor for $\epsilon^{\psi'}_{data}$, obtained from Monte Carlo (MC) simulation which accounts for the difference between the J/ψ events produced at rest and those produced from $\psi' \to \pi^+\pi^- J/\psi$. The correction factor in Eq. (1), which is approximately unity, is determined from

$$f_{cor} = \frac{\epsilon^{J/\psi}_{mc}}{\epsilon^{\psi'}_{mc}}, \quad (2)$$

where $\epsilon^{J/\psi}_{mc}$ is the detection efficiency of $J/\psi \to inclusive$ events determined from the J/ψ MC sample and $\epsilon^{\psi'}_{mc}$ is the efficiency determined from the $\psi' \to \pi^+\pi^- J/\psi$ ($J/\psi \to inclusive$) MC sample.

There are two major improvements over the method in Ref. [2]. One is the generalization of the $J/\psi \to$ 4-prong events to $J/\psi \to inclusive$ events, which allows the number of J/ψ events to be determined by requiring different numbers of charged tracks; the other is to use the MC samples of $J/\psi \to inclusive$ and $\psi' \to \pi^+\pi^- J/\psi$ ($J/\psi \to inclusive$) events generated with the BesEvtGen generator [3] based on GEANT4 [4] to determine the correction factor, f_{cor}. In this analysis, the events with more than one charged tracks are used to determine the number of J/ψ events.

At present only about 50% of the J/ψ decays are observed and listed in the Particle Data Group tables (PDG) [5]. In the MC simulation package, the unknown J/ψ decays are roughly generated with the Lundcharm model. In the Lundcharm model, charmonium decay via gluons is described by the QCD partonic theory, and the partonic hadronization is handled by the LUND model. Extended C- and G-parity conservation are assumed and abnormal suppression effects of charmonium decay are included [6].

II. $J/\psi \to inclusive$ SELECTION CRITERIA

Event selection criteria are required to distinguish $J/\psi \to inclusive$ events from Bhabha ($e^+e^- \to e^+e^-$), dimuon ($e^+e^- \to \mu^+\mu^-$), cosmic ray and beam-gas events in J/ψ data.

At the track level, candidate events are required to satisfy the following selection criteria:

1. Charged tracks are reconstructed using hits in the Main Drift Chamber (MDC) and are required to be in the polar angle range $|\cos\theta| < 0.93$, have momentum $p < 2.0$ GeV/c, and have the point of closest approach of the track to the beamline within 15 cm of the interaction point along the beam direction (V_z) and within 1 cm in the plane perpendicular to the beam (V_r).

2. Clusters in the electromagnetic calorimeter (EMC) must have at least 25 (50) MeV of energy in the barrel (end cap) EMC, have $|\cos\theta| < 0.83$ in the barrel ($0.86 < |\cos\theta| < 0.93$ in the endcap), and have EMC cluster timing T in the range of $0 < T < 15$ (with unit of 50 ns) to suppress electronic noise and energy deposits unrelated to the event.

At the event level, at least two charged tracks are required, and the visible energy, E_{vis}, must be greater than 1.0 GeV. Here E_{vis} is defined as the sum of charged particle energies computed from the track momenta by assuming pion masses and the neutral shower energies deposited in the EMC. According to the distribution of visible energy shown in Fig. 1, this requirement removes

two thirds of background events, estimated with the continuum data taken at the center-of-mass energy of 3.08 GeV, while it has little effect on the inclusive events.

To remove background from Bhabhas and dimuons, events with only two charged tracks must have the momenta of both charged tracks less than 1.5 GeV/c. Fig. 2 displays the scatter plot of the momenta of two charged tracks, where the clear cluster with the momenta around 1.55 GeV/c corresponds to the contribution from leptonic pairs. Most of the leptonic pairs are removed by the above requirement as indicated by the solid lines in Fig. 2. From the deposited energy distribution of charged tracks in the EMC, shown in Fig. 3, a peak around 1.5 GeV is clearly observed, which corresponds to the contribution of Bhabha events. Therefore, to further remove Bhabha events, the deposited energy in the EMC of each charged track is required to be less than 1 GeV. After the momentum and energy selections there remain 174.28 ± 0.01 million events (N_{sel}) from the J/ψ data. The distributions of the track parameters for closest approach and track angle V_r, V_z, $\cos\theta$,

the total energy deposited in the EMC (E_{emc}), and the charged multiplicity (N_{good}) after subtracting background events estimated with the continuum data taken at the center-of-mass energy of 3.08 GeV (see Section III for details) are shown in Figs. 4 through 8, respectively. Also shown are the distributions from MC simulation, normalized to J/ψ data. The distributions of V_z, V_r, and $\cos\theta$ of charged tracks, and the E_{emc} distribution for MC simulation are in reasonable agreement with those from data.

For the charged multiplicity distribution shown in Fig. 8, neither the MC simulation with the Lundcharm model nor the MC simulation without the Lundcharm model agree very well with the data. However the effect of this discrepancy between data and MC simulation on the correction factor is very small, as described in Section VII.

III. BACKGROUND ANALYSIS

Background events come mainly from Quantum Electro-Dynamics (QED) processes, beam-gas interactions, and cosmic rays. In this analysis, all of them are estimated with the number of events selected from the continuum data taken at the center-of-mass energy of 3.08 GeV, normalized to the J/ψ data after taking into account the energy-dependent cross section of the QED process:

$$N_{bg} = N_{3.08} \times \frac{\pounds_{J/\psi}}{\pounds_{3.08}} \times \frac{s_{3.08}}{s_{J/\psi}}, \qquad (3)$$

where N_{bg} is the estimated number of background events in the selected J/ψ events; $N_{3.08}$ is the number of events selected from the continuum data; $\pounds_{J/\psi}$ and $\pounds_{3.08}$ are the integrated luminosities for J/ψ and continuum data, respectively; $\sqrt{s_{J/\psi}}$ and $\sqrt{s_{3.08}}$ are the center-of-mass energies for J/ψ data (3.097 GeV) and the continuum data (3.080 GeV).

The integrated luminosities are determined using $e^+e^- \to \gamma\gamma$ events with the following selection criteria: there are at least two neutral tracks with the deposited energy of the second most energetic shower larger than 1.2 GeV and less than 1.6 GeV; and $|\cos\theta| < 0.8$, where θ is the polar angle in the EMC. The number of signal events is determined by counting in the signal region $|\Delta\phi| < 2.5°$ and the background estimated in the sideband region $2.5 < |\Delta\phi| < 5°$, where $\Delta\phi = |\phi_{\gamma 1} - \phi_{\gamma 2}| - 180°$ and ϕ is the angle of photon in x-y plane. Figs. 9 and 10 show the distribution of energy deposited in EMC and $\cos\theta$ of photons. The integrated luminosities of J/ψ data and continuum data are determined to be 79631 ± 70 ($stat.$) nb^{-1} and 281 ± 4 ($stat.$) nb^{-1}, respectively. Here, the statistic error is 1.5%, and the systematic error can be cancelled according to Eqs. 3.

With the same selection criteria for inclusive events

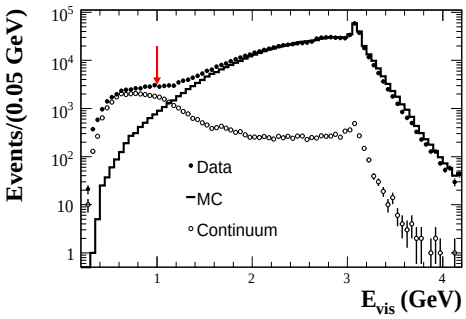

FIG. 1. The visible energy distributions for J/ψ data (dots with error bars), continuum data (circles with error bars) and MC simulation of $J/\psi \to inclusive$ events (histogram). The arrow indicates the minimum E_{vis} required to select inclusive events.

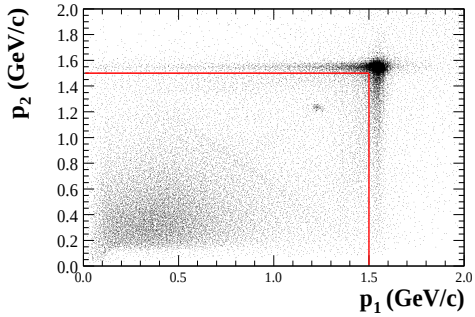

FIG. 2. The scatter plot of the momenta of the charged tracks for 2-prong events. The cluster around 1.55 GeV/c corresponds to the contribution from leptonic pairs. Most are removed with the requirements on the two charged tracks, $p_1 < 1.5$ GeV/c and $p_2 < 1.5$ GeV/c, as indicated by the solid lines.

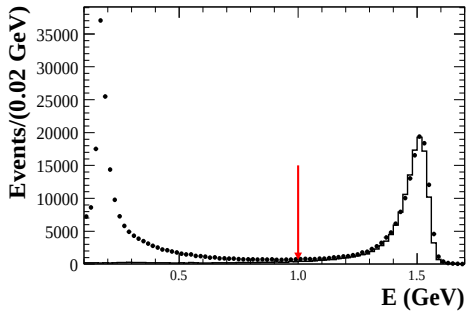

FIG. 3. The distributions of deposited energy in the EMC by the charged tracks of 2-prong events for J/ψ data (dots with error bars) and for the combined, normalized MC simulations of $e^+e^- \to e^+e^-$ and $J/\psi \to e^+e^-$ (histogram).

from J/ψ data, 21266 ± 146 events are selected from the continuum data. Therefore the number of background events (N_{bg}) is estimated to be 5.96 ± 0.04 million using Eq. (3). The background ratio in the selected $J/\psi \to inclusive$ events is calculated to be 3.5% by comparing the number of background events to the number of inclusive events selected from J/ψ data.

In the above calculation, the background events from cosmic rays and beam-gas interaction are normalized with the same procedure as QED events. In fact, the number of cosmic rays is proportional to the data taking time, whereas beam-gas events are related with the vacuum status and the beam current for taking data, in addition to the data taking time. In this analysis, the difference of the number of background events estimated with and without considering the energy dependence of the cross section for QED processes is taken into account in the overall systematic uncertainty of the number of J/ψ events (see Section VII for details).

IV. DETERMINATION OF THE DETECTION EFFICIENCY AND CORRECTION FACTOR

Usually the detection efficiency is determined using a MC simulation of $J/\psi \to inclusive$, assuming that the detector response is well simulated. The efficiency is then the ratio between the number of events detected and the number of events generated. In this analysis to avoid the uncertainty caused by any discrepancy between MC simulation and data, the detection efficiency is determined experimentally using 106 million ψ' events taken with the BESIII detector. The experimental detection efficiency, $\epsilon^{\psi'}_{data}$, is then the number of selected events divided by all $J/\psi \to inclusive$ events obtained from the cascade decays of $\psi' \to \pi^+\pi^- J/\psi$.

To select $\psi' \to \pi^+\pi^- J/\psi$ events, there must be at least two soft pions that are each reconstructed successfully in the MDC within the polar angle range $|\cos\theta| < 0.93$, have $V_r < 1$ cm and $|V_z| < 15$ cm, and have momentum less than 0.4 GeV/c. The π momentum distributions in Fig. 11 show that the MC simulation is in good agreement with data. There are no other requirements on the remaining charged and neutral tracks. The invariant masses recoiling against all possible $\pi^+\pi^-$ pairs are calculated and shown in Fig. 12. A clear peak around 3.1 GeV/c^2, corresponding to the decay of $\psi' \to \pi^+\pi^- J/\psi$, $J/\psi \to inclusive$, is observed over a large flat background. The number of $J/\psi \to inclusive$ events, $N_{inc} = (19526 \pm 10) \times 10^3$, is obtained by a fit to the $\pi^+\pi^-$ recoil mass spectrum with a double-Gaussian plus a second order Chebychev background function.

To determine the number of selected $J/\psi \to inclusive$ events, in addition to the above common selection criteria for the two soft charged pions, the remaining charged tracks and neutral tracks must satisfy the requirements for the $J/\psi \to inclusive$ events described in Section III. Fig. 13 shows the invariant mass recoiling against $\pi^+\pi^-$ for the selected events, and the number of selected $J/\psi \to inclusive$ events, N^{sel}_{inc}, is determined to be $(14432 \pm 9) \times 10^3$ from a fit with a double-Gaussian plus

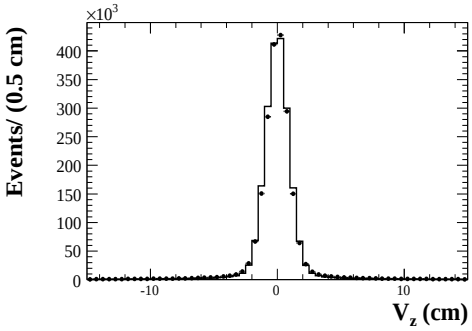

FIG. 4. The distributions of V_z for J/ψ data (dots with error bars) and MC simulation of $J/\psi \to inclusive$ (histogram).

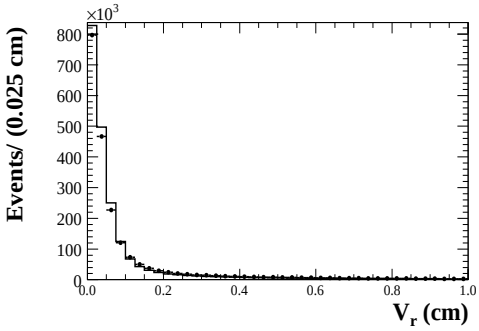

FIG. 5. The distributions of V_r for J/ψ data (dots with error bars) and MC simulation of $J/\psi \to inclusive$ (histogram).

a second order Chebychev background function. Finally the experimental detection efficiency of $J/\psi \to inclusive$ events, $\epsilon^{\psi'}_{data}$, is determined to be $(73.91 \pm 0.02)\%$.

Since the J/ψ decays in flight, a correction factor defined as in Eq. (2) is used to correct for the kinematical effect in order to determine the detection efficiency for direct $e^+e^- \to J/\psi \to inclusive$ decays. With the same procedure, including the event selection criteria and the fit functions, the detection efficiency of $\epsilon^{\psi'}_{mc} = (75.87 \pm 0.06)\%$, is obtained from a MC sample of 2 million of $\psi' \to \pi^+\pi^- J/\psi$ events. To determine $\epsilon^{J/\psi}_{mc}$, a MC sample of 1 million events of $J/\psi \to inclusive$ was generated. With the same selection criteria for $J/\psi \to inclusive$ events as listed in Section II, 766893 ± 423 events are selected, and the corresponding detection efficiency is calculated to be $(76.69 \pm 0.04)\%$. The correction factor f_{cor} for the detection efficiency, is then determined to be

$$f_{cor} = \frac{\epsilon^{J/\psi}_{mc}}{\epsilon^{\psi'}_{mc}} = 1.0108 \pm 0.0009. \quad (4)$$

V. TRIGGER EFFICIENCY

The trigger efficiency of the BESIII detector has been studied using different physics channels [7] and was found to be very close to 100%. Therefore, we do not repeat a similar study here, but assume a 100% trigger efficiency.

VI. THE NUMBER OF J/ψ EVENTS

The values of different parameters used in Eq. (1) are summarized in Table I, and the number of J/ψ events is then calculated to be $(225.30 \pm 0.02) \times 10^6$. Here the statistical error is only from N_{sel}, while the statistical fluctuation of N_{bg} is taken int account as part of the systematic uncertainties (see subsection 7.4). The systematic errors from different sources will be discussed in the next section in detail.

VII. SYSTEMATIC UNCERTAINTY

A. MC model uncertainty

The efficiency correction factor (f_{cor}), which is used to correct the detection efficiency for the in-flight J/ψ decay from ψ' data, is a MC simulation dependent parameter.

To check the MC model dependence of the correction factor, we also determine the correction factor with MC samples generated without the Lundcharm model. The difference of the correction factors obtained with and without the Lundcharm model, 0.49%, is taken as the systematic uncertainty from the MC model in the determination of the number of J/ψ events.

B. Tracking efficiency

According to tracking efficiency studies, the consistency of tracking efficiencies between MC simulation and data in J/ψ decays is 1% for each charged track, although it is a little larger at low momentum.

In this analysis, the consistency of tracking efficiency between MC simulation and data in ψ' decays is assumed to be the same as that in J/ψ decays. Actually there may be a difference in the two data sets taken at different center-of-mass energies. To estimate the corresponding uncertainty, the tracking efficiency in the J/ψ MC sample was varied by -0.5% for the tracks with momentum greater than 350 MeV/c and -1.0% for the tracks with momentum less than 350 MeV/c. The change of the correction factor due to this variation leads to a change of 0.40% in the number of J/ψ events, which is taken as the systematic uncertainty due to the tracking efficiency.

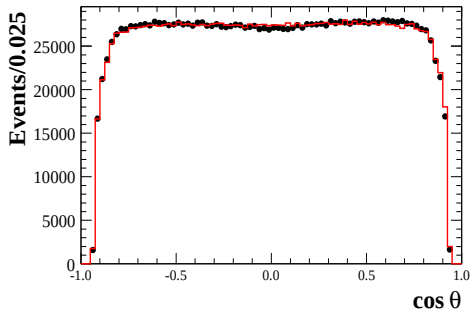

FIG. 6. The $\cos\theta$ distributions of charged tracks for J/ψ data (dots with error bars) and MC simulation of $J/\psi \to inclusive$ (histogram).

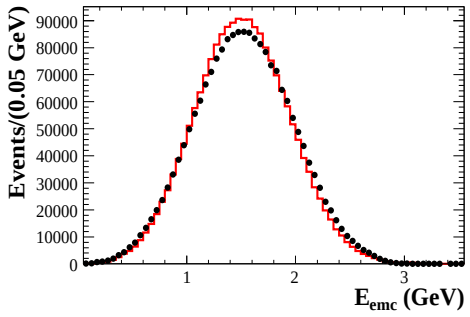

FIG. 7. The distributions of the total energy deposited in the EMC of $J/\psi \to inclusive$ events for J/ψ data (dots with error bars) and MC simulation (histogram).

C. Fitting of J/ψ peak

From the fit of the J/ψ peak we obtain the fitting errors 0.03% and 0.08% in the determination of $\epsilon^{\psi'}_{data}$ and $\epsilon^{\psi'}_{mc}$, respectively, In addition, the uncertainties caused by changing the signal function, background shape, and the fitting range in the fit of the invariant mass spectra recoil $\pi^+\pi^-$ are also taken into account. To estimate the uncertainty caused by a change of the signal function, we also fit the J/ψ peak with the J/ψ histogram shape, which is obtained from the recoil mass spectrum of $\pi^+\pi^-$ in $\psi' \to \pi^+\pi^- J/\psi,\ J/\psi \to \mu^+\mu^-$. The change of the result is just 0.04%. The uncertainty by changing the background shape from a second order Chebychev function to a first order one is less than 0.16%. If the fitting range is changed from [3.07, 3.13] GeV/c^2 to [3.08, 3.12] GeV/c^2, the change is 0.32%. The total systematic uncertainty from the fitting, 0.37%, is the sum of these errors in quadrature.

D. Background uncertainty

In the calculation of the number of J/ψ events, the background events from QED processes, cosmic rays and beam-gas events are estimated by normalizing the selected continuum events by the integrated luminosities according to Eq. (3). Therefore the statistical error of the number of events selected from the continuum data, 0.69% and the uncertainties due to the measurement of the integrated luminosities of the J/ψ data and continuum data, 1.5%, must be taken into account in the background uncertainty.

As discussed in Section 3, normalizing cosmic rays and beam-gas events with the energy-dependent factor for QED processes is not correct. To account for this, the difference, 1.1%, between the determinations of the background normalized with and without the energy-dependent factor is taken as a background uncertainty.

To estimate the background uncertainty from the beam-gas events, we select samples of beam-gas events in the J/ψ and continuum data. The candidate beam-gas events must have one or two charged tracks with the points of closest approach satisfying $|V_z| > 5$ cm and $|V_z| < 15$ cm and the visible energy less than 0.5 GeV. 26844720 events are selected from the J/ψ data, corresponding to 93470 events expected in the continuum data by normalizing with the integrated luminosities. Compared with 96230 beam-gas events directly selected from the continuum data, the difference between them, 3%, is taken as a background uncertainty.

By adding all the above effects in quadrature, the total background uncertainty is 3.6%. Since the background ratio in $J/\psi \to inclusive$ events is 3.5%, the systematic uncertainty in the number of J/ψ events is 0.13%.

E. Dependence on charged multiplicity

In order to reduce the number of beam-gas events in this analysis, the selected $J/\psi \to inclusive$ events are required to have at least two good charged tracks ($N_{good} \geq 2$). The uncertainty from this requirement is estimated by varying the charged multiplicity requirement from $N_{good} \geq 2$ to $N_{good} \geq 3$. For comparison, the values obtained for the two cases are listed in Table II. The change of the number of J/ψ events, 0.76%, is taken as the systematic uncertainty of the charged multiplicity requirement.

F. Noise mixing

Noise in the BESIII detector has been included in the realization of MC simulation by mixing in noise from events recorded using a random trigger for both J/ψ and ψ' data. To determine the systematic error associated

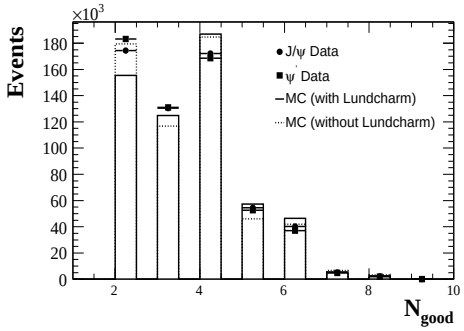

FIG. 8. The distributions of the charged multiplicity of $J/\psi \to inclusive$ events for J/ψ data (dots with error bars) and ψ' data (squares with error bars) and MC simulation generated with and without the Lundcharm model (solid and dashed histograms, respectively).

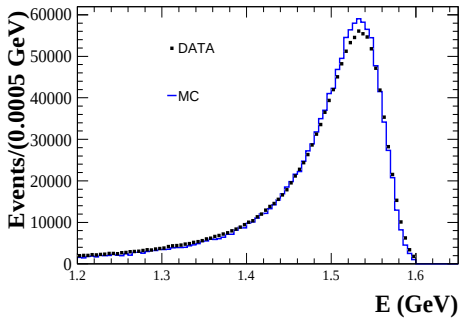

FIG. 9. The distributions of deposited energy in EMC of photon in $e^+e^- \to \gamma\gamma$ for data (dots) and MC simulation (histogram).

with the noise realization in MC simulation, the ψ' MC sample is reconstructed with the higher noise from J/ψ data, and the change of the detection efficiency correction factor, 0.4%, is taken as a systematic uncertainty in the determination of the number of J/ψ events.

In this analysis 106 million of ψ' events are used to determine the detection efficiency. However, the noise level was not entirely stable during the period of ψ' data taking. To check the effect of the changing noise level on the detection efficiency, the ψ' data and the MC sample are divided into three sub-samples, and the detection efficiency is determined for each of the three samples. The change of the detection efficiency and the correction factor lead to a change in the number of J/ψ events. The maximum change, 0.28%, is taken as the systematic uncertainty associated with the changing noise levels. The total systematic uncertainty from the noise mixing effect is estimated to be 0.49% by adding the individual error contributions in quadrature.

G. Estimation of $N_{J/\psi}$ with the sideband of $\bar{V}_z$

The reliability of the determination of the number of J/ψ events obtained from the above method is checked by applying another method entailing two different procedures. One difference concerns the selection of inclusive events, which is essentially the same as in Section 2. except for the requirement on the track vertex position V_z along the beam direction. Here we determine the average position $\bar{V}_z$ of the charged tracks. The signal region for inclusive events is defined by $|\bar{V}_z| < 4$ cm. This requirement is also applied in the determination of the detection efficiency and the correction factor. The $\bar{V}_z$ distribution is shown in Fig. 14.

The second difference is in the background estimation. The numbers of background events from cosmic rays and beam-gas interactions are estimated from the $\bar{V}_z$ sideband, defined by $6 < |\bar{V}_z| < 10$ cm. The subtraction of the sideband events from the events in the signal region removes the cosmic ray and beam-gas events.

The sideband subtraction does not account for the QED background events since the V_z distribution is similar to that of inclusive events from J/ψ decays. However the continuum data allows us to estimate the contribution of QED processes in the inclusive events selected from J/ψ data. The same event selection is applied to the continuum data to select the QED events. After subtracting the cosmic rays and beam-gas events estimated with the same sideband method as for J/ψ data, the amount of background events from the QED processes in the selected inclusive events is estimated by normalizing according to the integrated luminosities of the continuum and J/ψ data according to Eq. (3).

The same procedures have been used to determine the detection efficiency from ψ' data and the correction factor with MC samples. At last, the number of J/ψ events is determined to 224.9 million. The change in the number of J/ψ events with respect to the previous method discussed in chapter 6 is 0.20% and is taken as a systematic uncertainty.

H. Selection efficiency uncertainty of two soft pions

According to a MC study, the selection efficiency of soft pions, $\epsilon_{\pi^+\pi^-}$, recoiling against J/ψ in $\psi' \to \pi^+\pi^- J/\psi$ depends on the multiplicity of the J/ψ decay. To study its effect on the determination of the number of J/ψ events, $\psi' \to \pi^+\pi^-(\pi^0\pi^0)J/\psi$, $J/\psi \to \mu^+\mu^-, 2(\pi^+\pi^-)$ events are selected from data and inclusive MC samples, and then re-weighting factors are determined for J/ψ decaying into different multiplicities by comparing the corresponding selection efficiency of soft pions between data and MC. The difference between the results with and without re-weighting, 0.34%, is taken as the uncertainty due to the selection efficiency uncertainty of the soft pions in $\psi' \to \pi^+\pi^- J/\psi$.

The systematic uncertainties from different sources studied above are listed in Table III. The total systematic uncertainty, 1.24%, is the sum of them added in quadra-

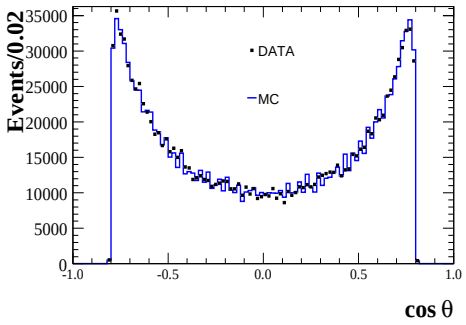

FIG. 10. The $\cos\theta$ distributions of photon in $e^+e^- \to \gamma\gamma$ for data (dots) and MC simulation (histogram).

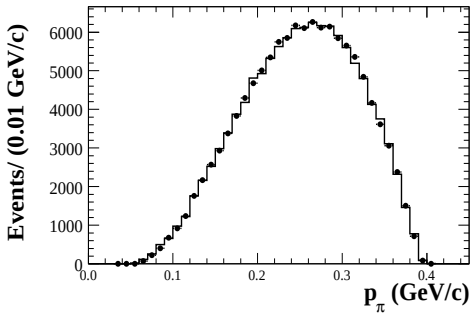

FIG. 11. The π momentum distributions from ψ' data (dots with error bars) and MC simulation of $\psi' \to \pi^+\pi^- J/\psi$, $J/\psi \to \mu^+\mu^-$ (histogram).

ture.

VIII. SUMMARY

Using $J/\psi \to$ *inclusive* events, the number of J/ψ events collected with the BESIII detector in 2009 is determined to be

$$N_{J/\psi} = (225.3 \pm 2.8) \times 10^6, \quad (5)$$

where the error is the systematic error and the statistical one is negligible.

ACKNOWLEDGMENTS

The BESIII collaboration thanks the staff of BEPCII and the computing center for their hard efforts. Supported in part by the Ministry of Science and Technology of China under Contract No. 2009CB825200; National Natural Science Foundation of China (NSFC) under Contracts Nos. 10625524, 10821063, 10825524, 10835001, 10935007, 11125525; Joint Funds of the National Natural Science Foundation of China under Contracts Nos. 11079008, 11179007; the Chinese Academy of Sciences (CAS) Large-Scale Scientific Facility Program; CAS under Contracts Nos. KJCX2-YW-N29, KJCX2-YW-N45; 100 Talents Program of CAS;Istituto Nazionale di Fisica Nucleare, Italy; U. S. Department of Energy under Contracts Nos. DE-FG02-04ER41291, DE-FG02-91ER40682, DE-FG02-94ER40823; U.S. National Science Foundation; University of Groningen (RuG) and the Helmholtzzentrum fuer Schwerionenforschung GmbH (GSI), Darmstadt; WCU Program of National Research Foundation of Korea under Contract No. R32-2008-000-10155-0

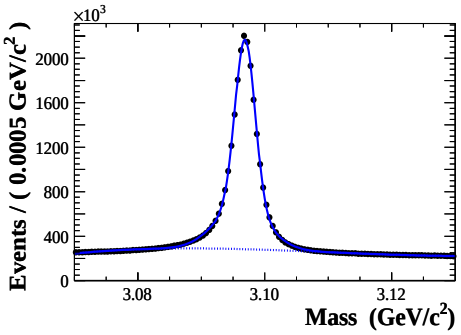

FIG. 12. The invariant mass recoiling against selected $\pi^+\pi^-$ pairs for ψ' data. A clear peak corresponding to $\psi' \to \pi^+\pi^- J/\psi$, $J/\psi \to$ *inclusive* is seen. The curves are the results of the fit described in the text.

[1] Medina Ablikim et al. Nucl. Instrum. Meth. A, 2010, **614**: 345-399
[2] Fang S S et al. HEP& NP, 2003, **27**: 277-281
[3] Ping R G Chinese Phys. C, 2008, **32**: 599-602
[4] Agostinellia S et al., Nucl. Instrum. Meth. A, 2003, **506**: 250-303
[5] Amsler-Gaume C et al., Phys. Lett. B, 2008, **667**: 1-5
[6] Chen J C et al., Phys. Rev. D, 2000, **62**: 1-8
[7] Berger N et al., Chinese Physics C, 2010, **34**: 1779-1784

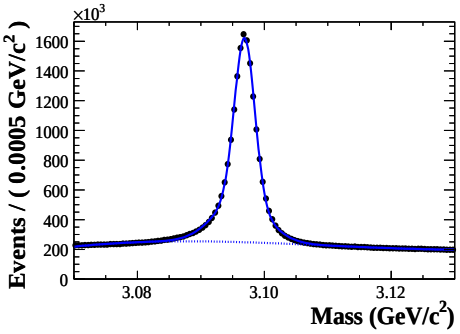

FIG. 13. The invariant mass recoiling against selected $\pi^+\pi^-$ pairs for ψ' data. Here, in addition to selection criteria on the pion pairs, the remaining portion of the event must satisfy the selection criteria for $J/\psi \to inclusive$ events. The curves are the results of the fit described in text.

TABLE I. The values of different parameters used in the calculation and the resulting number of J/ψ events.

item	value
N_{sel}	$(174.28 \pm 0.01) \times 10^6$
N_{bg}	$(5.96 \pm 0.04) \times 10^6$
ϵ_{trig}	1.00
$\epsilon^{\psi'}_{data}$	0.7391 ± 0.0002
$\epsilon^{\psi'}_{mc}$	0.7587 ± 0.0006
$\epsilon^{J/\psi}_{mc}$	0.7669 ± 0.0004
f_{cor}	1.0108 ± 0.0009
$N_{J/\psi}$	$(225.30 \pm 0.02) \times 10^6$

TABLE II. The number of J/ψ events and values used in the calculation for $N_{good} \geq 2$ and $N_{good} \geq 3$.

item	$N_{good} \geq 2$	$N_{good} \geq 3$
N_{sel}	174.28×10^6	119.89×10^6
N_{bg}	5.96×10^6	1.70×10^6
ϵ_{trig}	1.00	1.00
$\epsilon^{\psi'}_{data}$	0.7391	0.5050
$\epsilon^{\psi'}_{mc}$	0.7587	0.5451
$\epsilon^{J/\psi}_{mc}$	0.7669	0.5620
f_{cor}	1.0108	1.0310
$N_{J/\psi}$	225.3×10^6	227.0×10^6

TABLE III. Summary of systematic uncertainties on the number of J/ψ events.

Sources	Relative error (%)
MC model uncertainty	0.49
Tracking efficiency	0.40
Fitting of J/ψ peak	0.37
Background uncertainty	0.13
Multiplicity requirement	0.76
Noise mixing	0.49
Sideband method	0.20
$\epsilon_{\pi^+\pi^-}$ uncertainty	0.34
Total	1.24

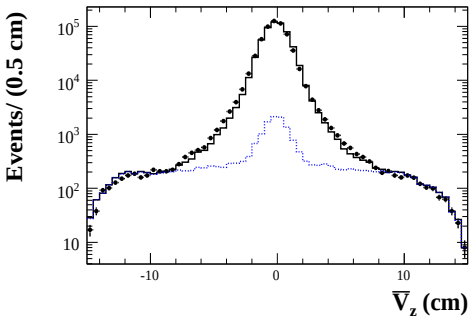

FIG. 14. The distributions of the average z vertex of charged tracks, $\bar{V}_z$, for J/ψ data (dots with error bars), MC simulation of $J/\psi \to$ *inclusive* plus continuum data (solid histogram) and continuum data (dashed histogram).